

Russian academy of Sciences
Kurnakov Institute of General and Inorganic Chemistry



**PROMISING ULTRA-HIGH-TEMPERATURE
CERAMIC MATERIALS
FOR AEROSPACE APPLICATIONS**

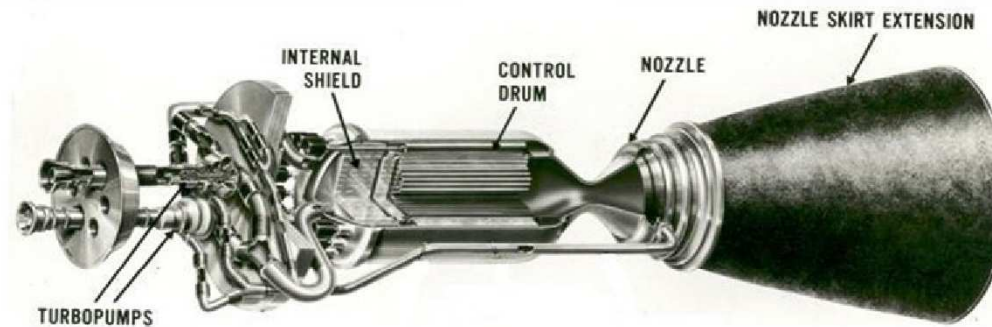
Academician N.T. Kuznetsov

Genova, 2017

- 1) *Directed selection of materials,*
- 2) *Development of methods for synthesizing high-temperature materials*



Perspective models of hypersonic vehicles

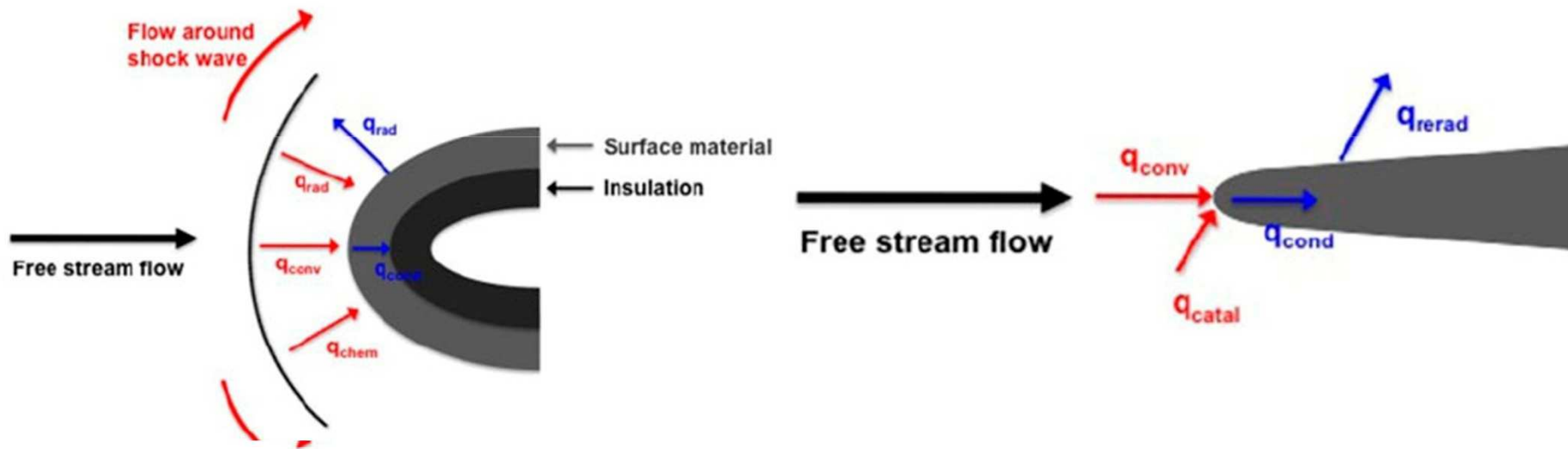


*Complex analysis of the row:
Molecule → Material → Technology → Products*

Interaction between Components with a Blunt and Sharp Edges and High-enthalpy High-Speed Dissociated Airflow

R – dozens of centimeters (Shuttle)

R – from millimeters to fraction



Requirements for Ultra-High-Temperature Composites

- High melting points
- High phase stability in a wide temperature range
- High oxidation stability including with atomic oxygen
- Low catalytic activity in the reactions of surface recombination
- Sufficiently high thermal conductivity
- High emissivity
- Sufficiently good mechanical properties

Refractory Components of Modern Construction

Ceramomatrix Materials and Coatings

Carbon	Carbon materials
Oxides	SiO ₂ , TiO ₂ , Al ₅ Y ₃ O ₁₂ , Al ₂ O ₃ , Y ₂ O ₃ , HfO ₂ , ZrO ₂ , Ln ₂ Zr ₂ O ₇ , Ln ₂ Hf ₂ O ₇ , ZrO ₂ -HfO ₂ -Y ₂ O ₃
Carbides	B ₄ C, SiC, TiC, ZrC, HfC, TaC, Ta ₄ ZrC ₅ , Ta ₄ HfC ₅
Nitrides	Si ₃ N ₄ , BN
Silicides	TaSi ₂ , HfSi ₂ , ZrSi ₂ , MoSi ₂
Borides	TiB ₂ , ZrB ₂ , HfB ₂

1700°C

Melting Point

~4000°C

Properties of Refractory Compounds

Comp.	ρ , g/cm ³	T_m , °C	λ , W/(m·K)	ε	LCTE·10 ⁶ , 1/K
SiC	3,2	2824 ¹	41,9 (20°C); 13,0 (1230°C)	0,8-0,85	4,7-5,5 (300-1773°C)
TaC	14,6	3983	22,0 (20°C); 29,1 (2230°C)	0,62-0,85	7,8 (25-2600°C)
HfC	12,7	3960	6,3 (25°C); 37,1 (2600°C)	0,77	7,54 (25-2600°C)
ZrB ₂	6,0	3040	58,0 (20°C); 134,0 (2000°C)	0,89-0,92	6,5 (1000-1700°C)
HfB ₂	11,2	3250	51,0 (20°C); 143,0 (2000°C)	0,89-0,91	6,8 (1000-1700°C)
ZrO ₂	5,65	2700 ²	1,9 (40 K); ~2 (1000-1300°C)	0,28-0,35	8-10,6 (1000°C)
HfO ₂	10,1	2800 ²	2-3 (200-2200°C)	0,6-0,8	6-9 (100-2500°C)

¹Decomposition, ²There are the phase transitions up to T_m

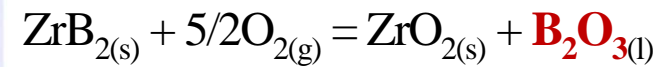
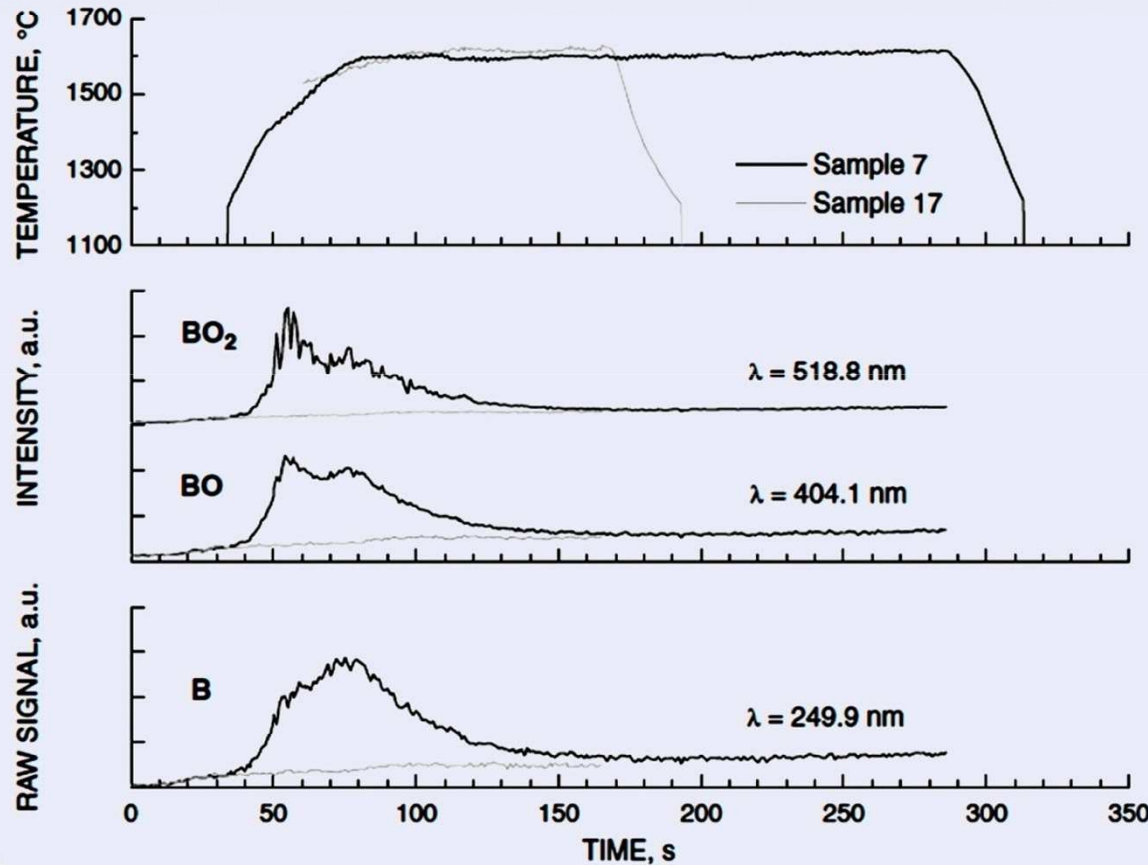
ρ – density

T_m – melting point

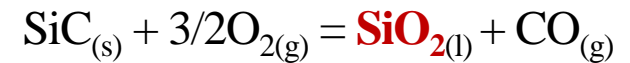
λ – thermal conductivity

LCTE – linear coefficient of thermal expansion

Oxidation of Materials Based on the ZrB₂ and HfB₂



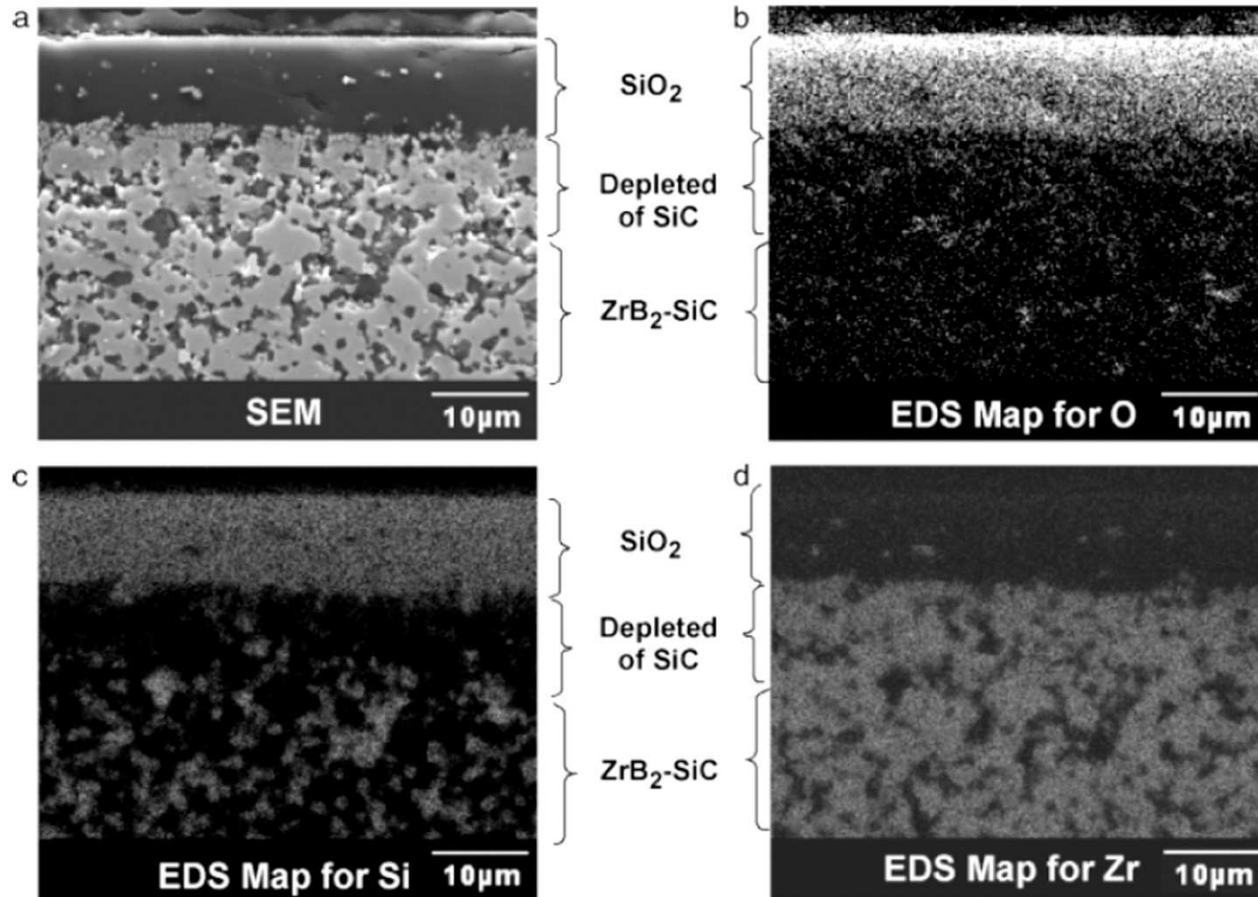
+SiC (>1000-1200°C):



$\text{SiO}_{2(l)} + \text{B}_2\text{O}_{3(l)} \Rightarrow$ **viscous borosilicate glass**

[M. Playez, Fletcher D.G., Marschall J. et al. // J. Thermophys. Heat Transfer. 2009. V. 23. №2. P. 279.]

Oxidation of Materials $ZrB_2(HfB_2)/SiC$: Formation of Multilayer Oxidized Region



Microstructure of the cut material ZrB_2 -30vol.%SiC (a) and the map of element distribution: O (b), Si (c), Zr (d) after its oxidation at 1500°C during 30 min.

[Fahrenholtz W.G. // *J. Am. Ceram. Soc.* 2007. V. 90. №1. P. 143]

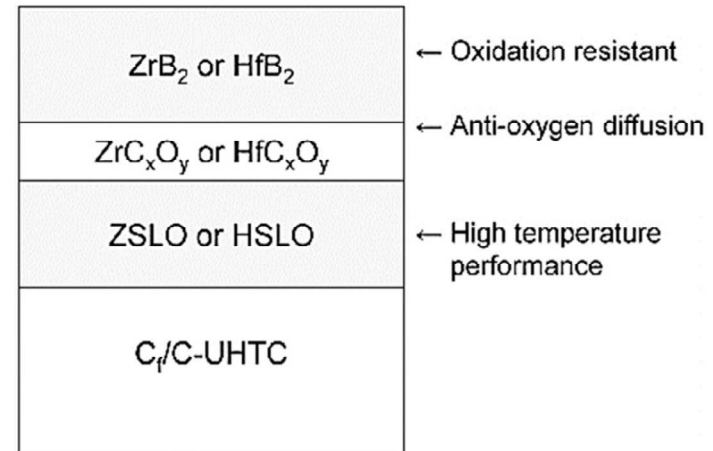
Ultra-refractory carbides

The introduction of the ultra-refractory carbides in the CM composites leads to:

- The inhibition of $\text{HfB}_2(\text{ZrB}_2)$ grain growth in the process of UHTC obtaining ($T \sim 1900\text{-}2200^\circ\text{C}$).
- The modification of the protective borosilicate glass composition, resulting on UHTC oxidation.
- The difficulty of the oxygen diffusion into the materials due to the oxycarbides formation.
- The optimization of mechanical properties.

TaC } High T_m , more refractory glass, the
 HfC } increased oxidation resistance (due to the
 ZrC } oxycarbide formation), the inhibition of
 diboride grain growth, improvement of
 mechanical properties

TiC - The glass modification (the increase of
 liquation phenomenon probability),
 improvement of mechanical properties,
 the stabilization of $\text{HfO}_2(\text{ZrO}_2)$, formed
 in the oxidation



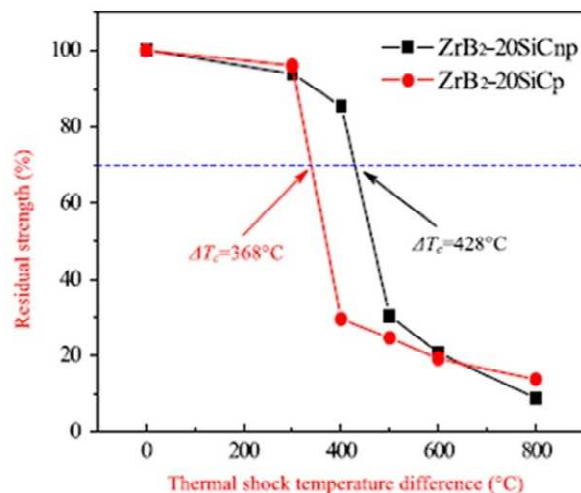
ZSLO – $\text{ZrB}_2/20 \text{ vol.}\% \text{ SiC} + (5\text{-}10 \text{ vol.}\% \text{ La}_2\text{O}_3)$
 HSLO – $\text{HfB}_2/20 \text{ vol.}\% \text{ SiC} + (5\text{-}10 \text{ vol.}\% \text{ La}_2\text{O}_3)$

Scheme of a multi-layered defense system on the Cf/C – composite surface

Silicon carbide

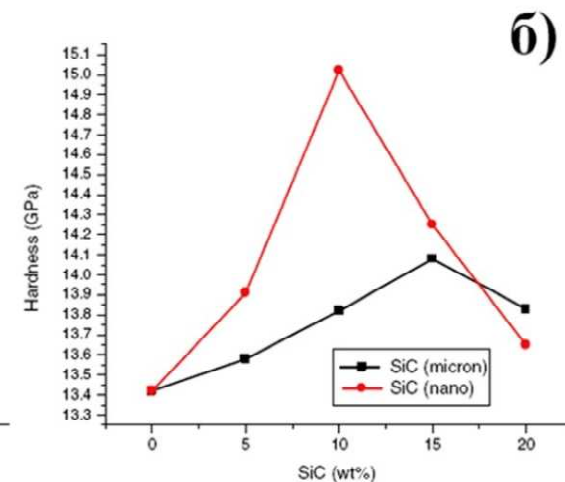
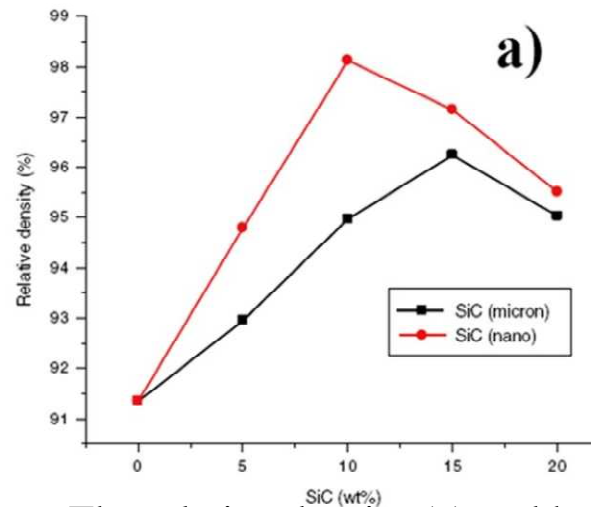
The use of nanosized SiC in obtaining UHTC $\text{HfB}_2(\text{ZrB}_2)/\text{SiC}$ leads to:

1. The improvement of the sintering process of CM.
2. The increasing of the oxidative stability of CM.
3. The optimization of the mechanical properties of CM.



The residual strength of the composites $\text{ZrB}_2/20\text{SiC}_p$ and $\text{ZrB}_2/20\text{SiC}_{np}$ (with nanoparticles SiC, black markers) depending on the temperature difference.

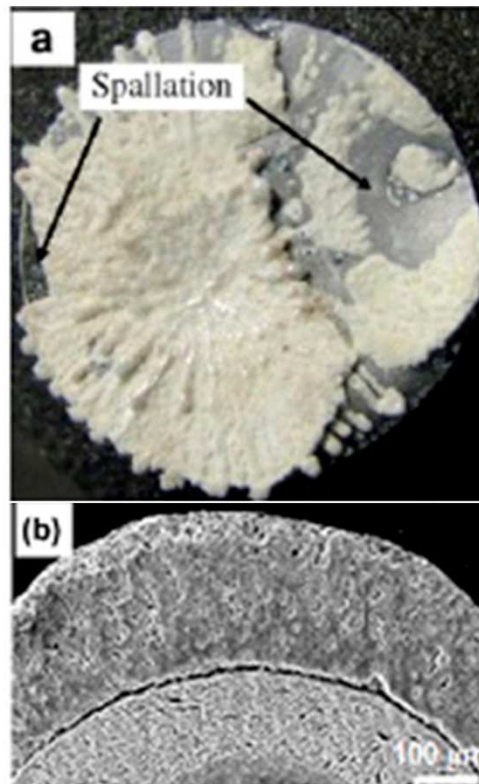
[Han W., Zhou S., Zhang J. // *Ceram. Int.* – 2014. – V. 40 – № 10 – P.16665–16669]



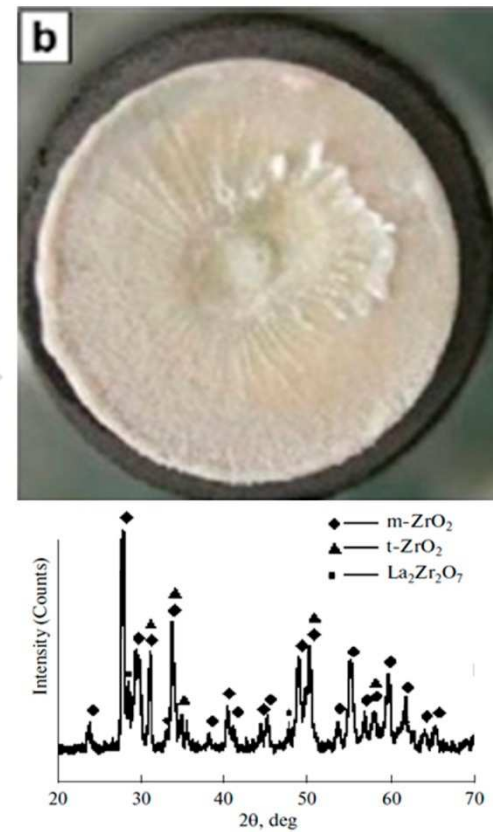
The relative density (a) and hardness (b) for samples obtained by pressing, followed by sintering at 2200°C (1 hour), depending on the SiC content: red markers –nanosized SiC, black markers–microsized SiC

[Mashhadi M., Khaksari H., Safi S. // *J. Mater. Res. and Technology* – 2015. – V. 4 – № 4 – P.416–422]

Partial stabilization of the ZrO_2 and HfO_2 , obtaining at the ZrB_2 and HfB_2 oxidation, by adding of the REE oxides or borides to the oxide charge to improve adhesion of the oxidized layer to the massive part of the sample



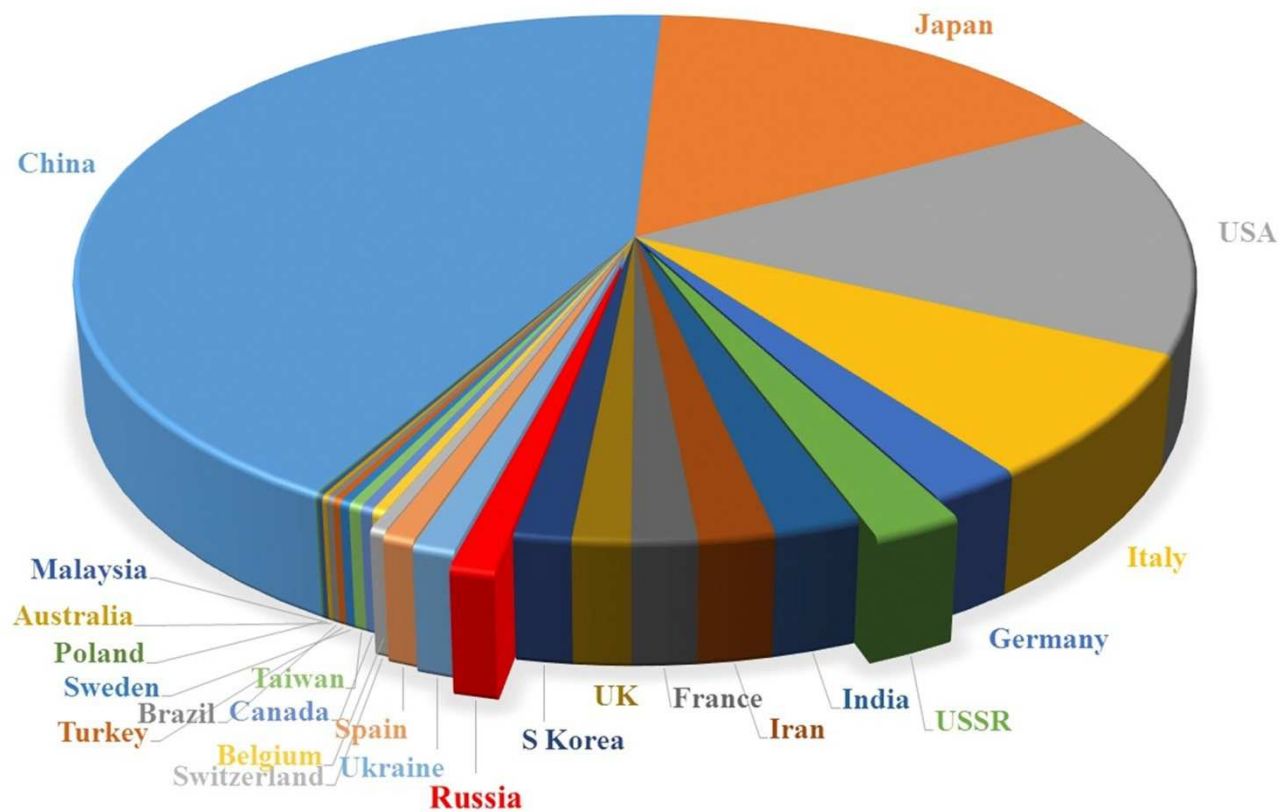
+ Ln_2O_3 ,
 LnB_6 , other
stable oxides



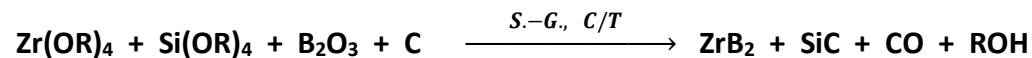
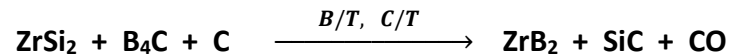
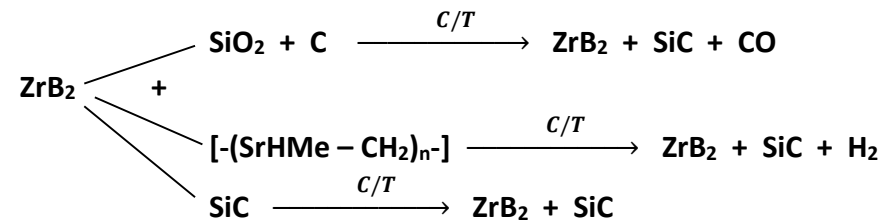
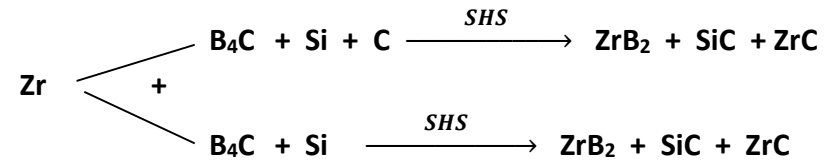
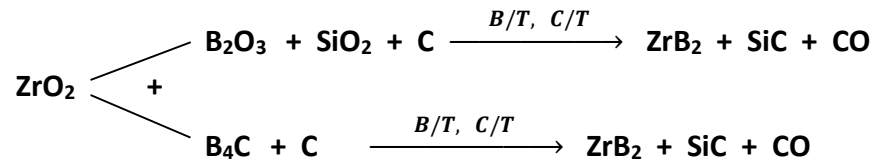
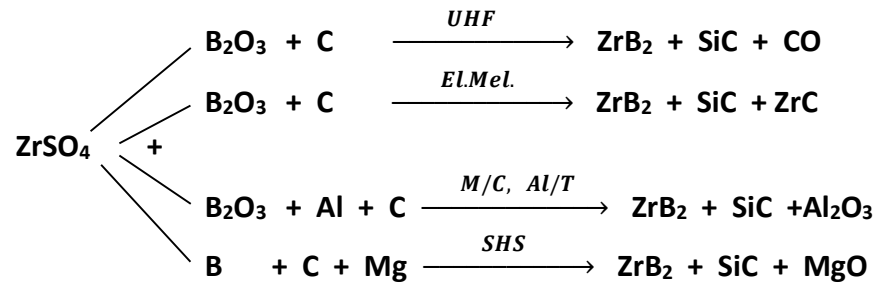
Exfoliation of oxides part

Jin X., He R., Zhang X. et al. // *J. Alloys Compd.* 2013. V. 566. P. 125.
Zhang X., Hu P., Han J. et al. // *Compos. Sci. Technol.* 2008. V. 68. P. 1718.

The distribution of publication on CM $ZrB_2(HfB_2)/SiC$ countries (SciFinder, STNInternational)



METHODS OF ZrB₂/SiC CM PREPARATION



SPS Synthesis of the UHTC HfB₂/xSiC

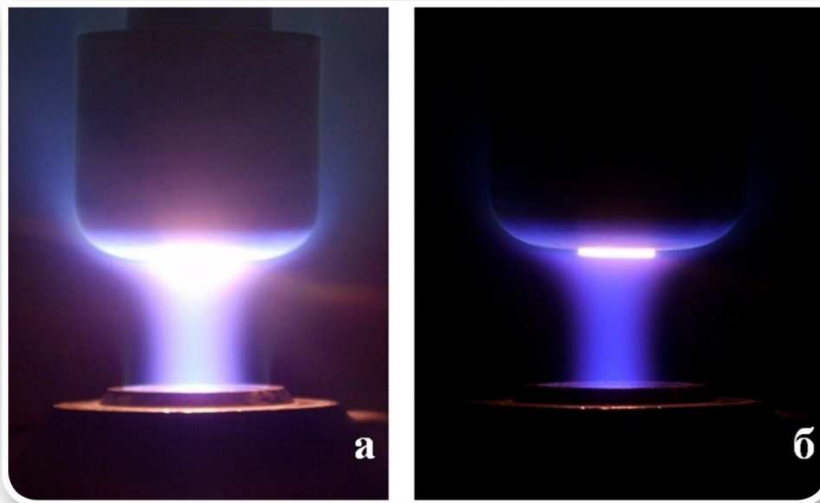
Series	Content SiC, vol. %	Density, g/cm ³	Porosity, %	Parameters of surface roughness, μm	
				R _a	R _y
1	25	6,1±0,2	29±3	0,71	3,93
2	35	5,6±0,2	28±2,5	0,64	4,68
3	45	5,9±0,1	18±1,5	1,58	6,24

Sevast'yanov V.G., Simonenko E.P., Gordeev A.N., Simonenko N.P., Kolesnikov A.F., Papynov E.K., Shichalin O.O., Avramenko V.A., Kuznetsov N.T. // Russian Journal of Inorganic Chemistry, 2013, Vol. 58, No. 11, pp. 1269–1276

Study of UHTC HfB₂/SiC (10-45 vol.% SiC) Behavior under the Action of the Dissociated Airflow



The HfB₂/SiC sample enshrined in the holder



The appearance of the plasmotron work

Test Mode

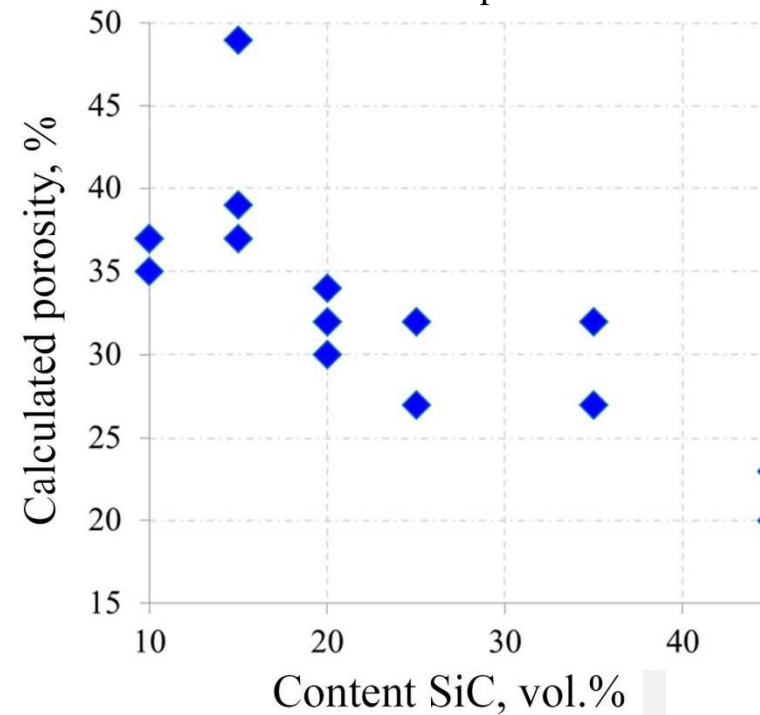
Power of the anode supply of plasmotron 45-64 kW
(for some samples 72 kW short);

Pressure in the pressure chamber of plasmotron
1-1,6 · 10⁻² MPa (for some samples 2 · 10⁻² MPa)

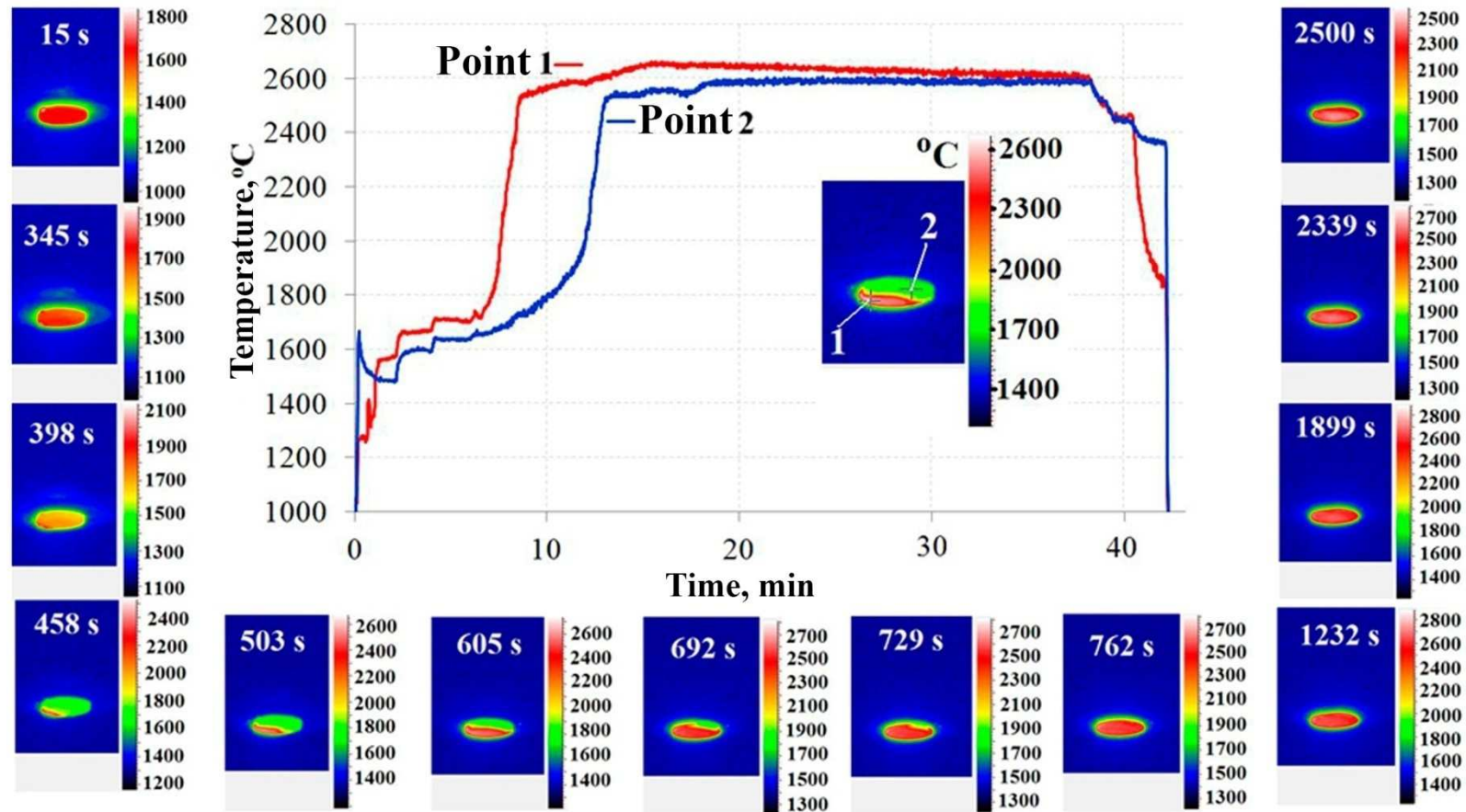
Enthalpy of a stream: 28,2-35,3 MJ/kg

Diameter of the nozzle: 30 mm

Distance to the sample: 30 mm

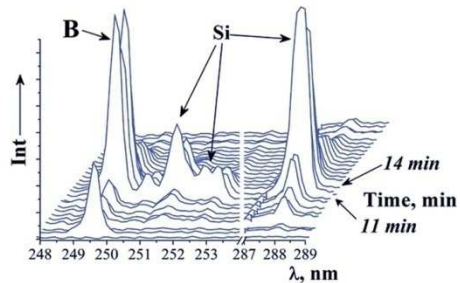


Study of the Behavior of UHTC HfB_2/xSiC under the Action of Dissociated Airflow ($x=10\text{--}45\text{vol.}\%$)

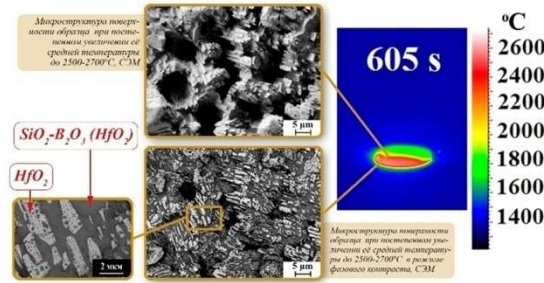


The temperature change of the sample surface of $\text{HfB}_2\text{-SiC}$ ceramics (15 vol.% SiC) in microdomains 1 and 2 in the experiment, and the thermoimages of the samples a surface in different time (according to the spectral pyrometer data)

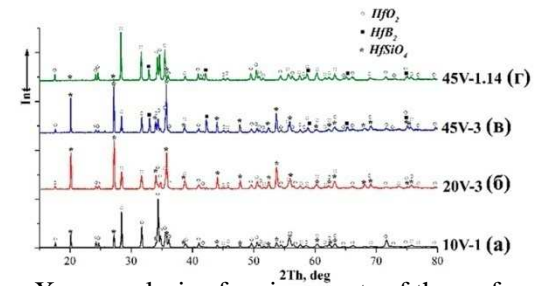
Study of the Behavior of UHTC HfB_2/xSiC under the Action of Dissociated Airflow ($x=10\text{--}45\text{vol.}\%$)



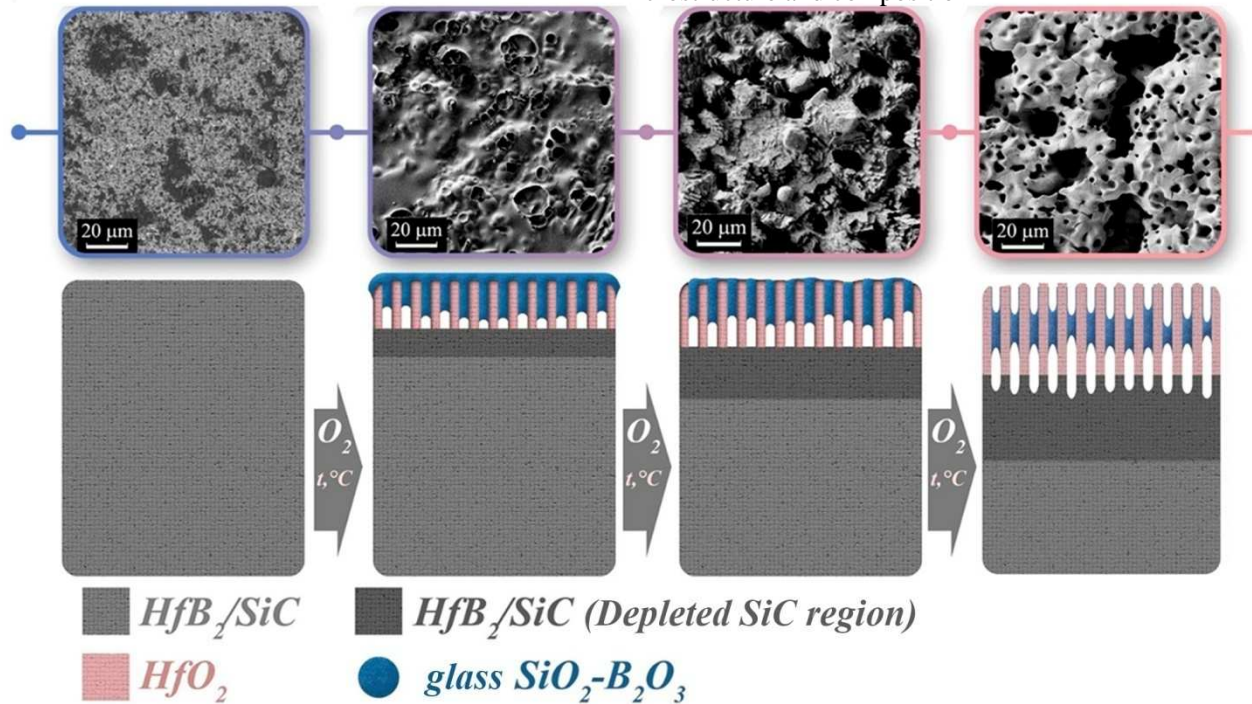
Emission spectroscopy of the boundary layer above the sample



Thermoimages of the sample surface under the high-enthalpy air stream action, and the study of their microstructure and composition

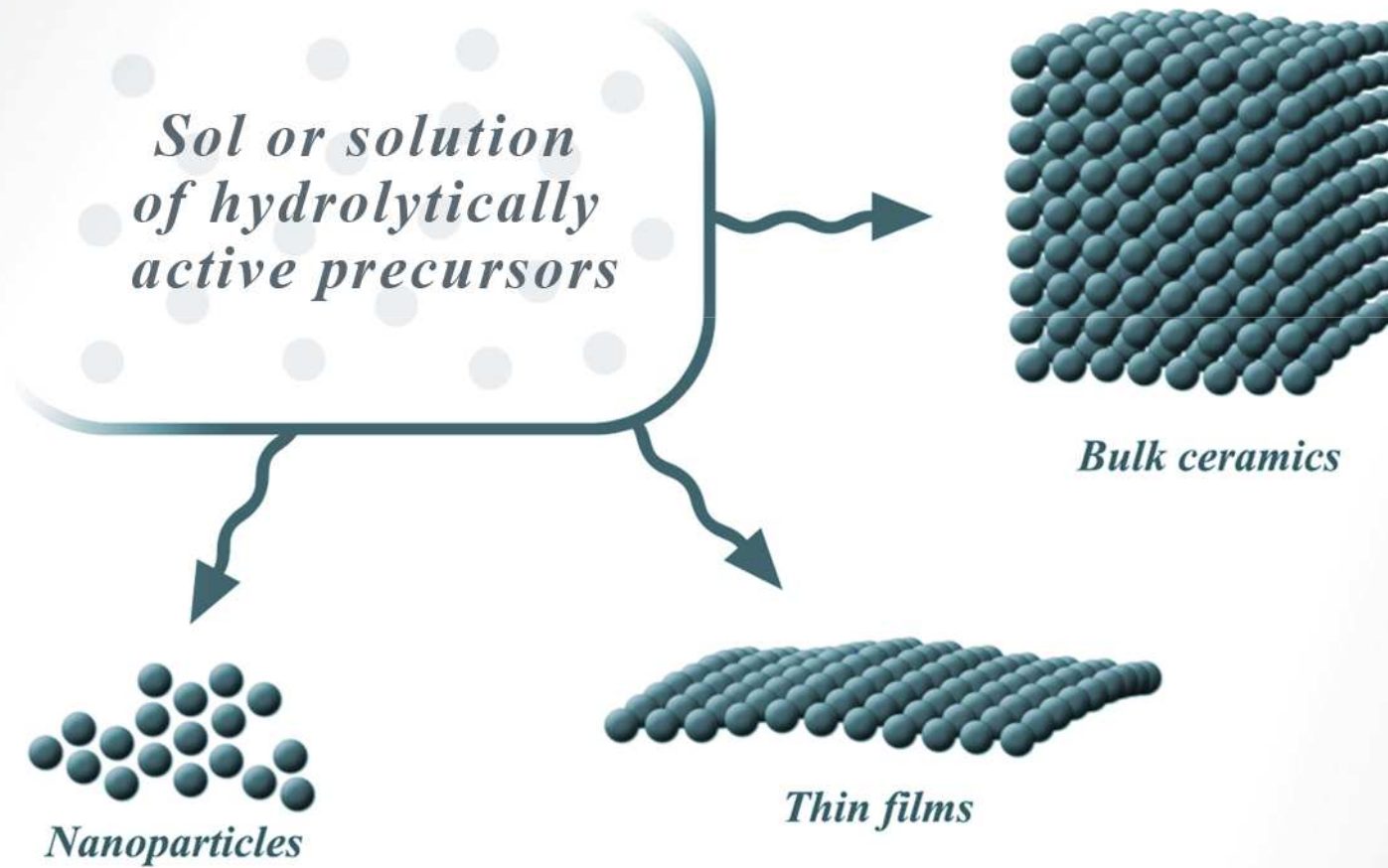


X-ray analysis of various parts of the surface after the action



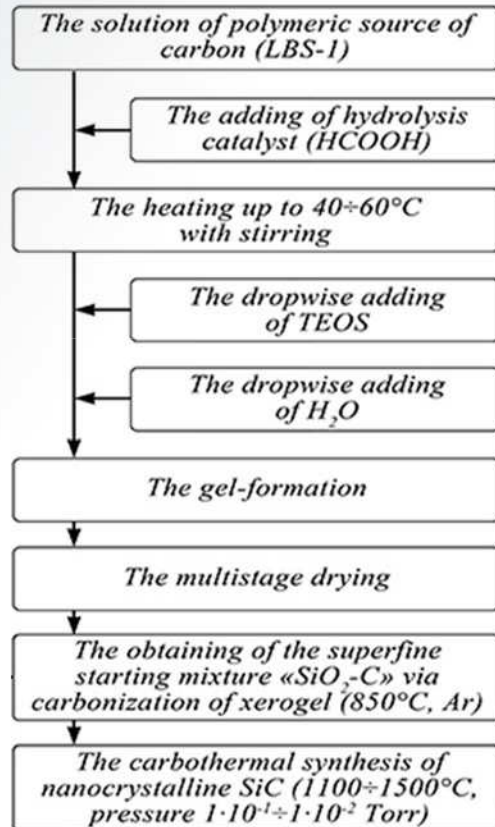
Changes in the composition and the microstructure of the HfB_2/SiC sample surface with prolonged action by high-enthalpy air stream

SOL-GEL TECHNOLOGY

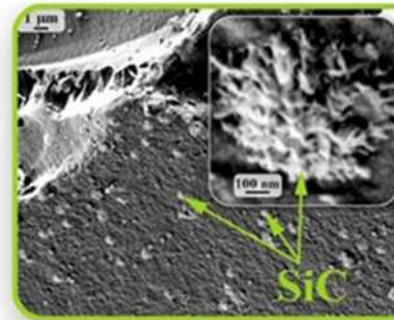


PREPARATION OF NANOSTRUCTURED SILICON CARBIDE USING SOL-GEL TECHNOLOGY

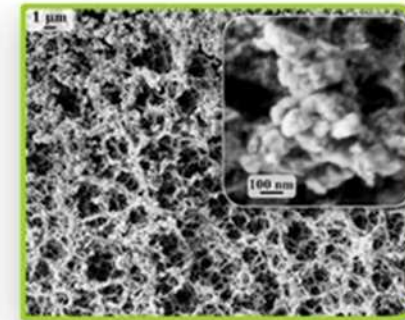
*Diagram for synthesis of superfine SiC directly in the bulk of SiC material using sol-gel technique**



Appearance of silicon & polymer-bearing gel



Microstructure of SiO₂-C-SiC samples, obtained by heat treatment under dynamic vacuum at the temperature of 1200 °C (exposure time of 5 h)



Microstructure of nanostructured SiC powder, obtained by heat treatment under dynamic vacuum at the temperature of 1500 °C (exposure time of 5 h)

**Jointly with Federal State Unitary Enterprise «All-Russian Scientific Research Institute of Aviation Materials»*

HIGHLY DISPERSED REFRACTORY CARBIDES

TiC, ZrC, HfC, TaC, Ta₄ZrC₅, Ta₄HfC₅

*Synthesis of precursors -
metal alkoxides and alkoxo-
acetylacetonates*

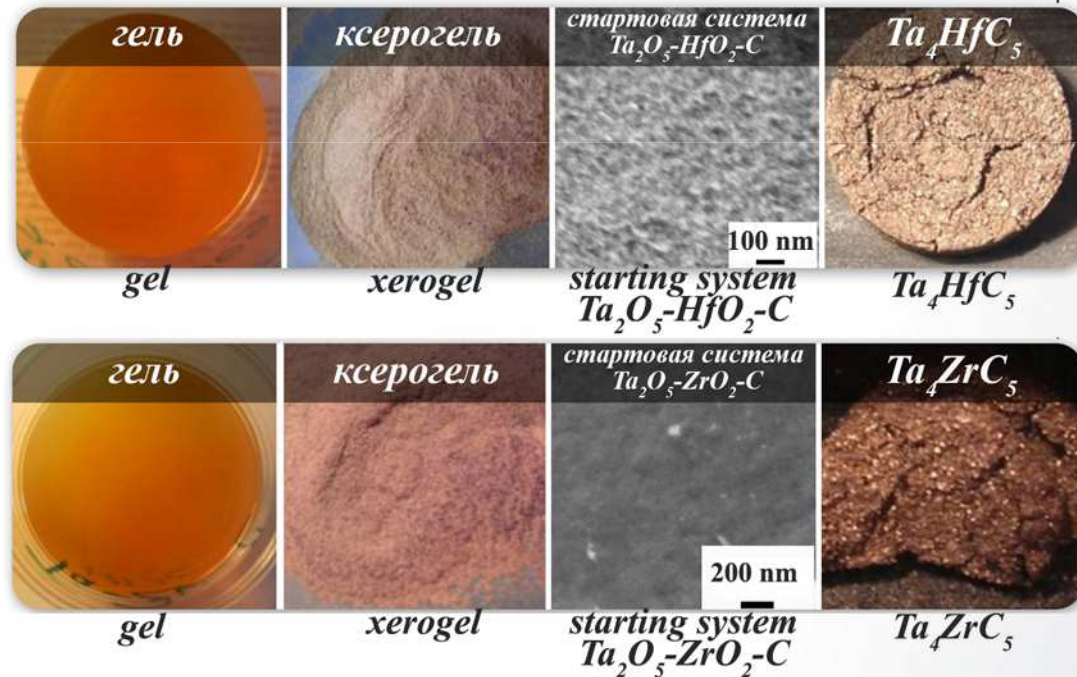
*Hydrolysis and gelation
in the presence of a polymeric
carbon source*

*Gel drying and heat pretreatment →
pyrolysis of the resin and formation of a
highly dispersed system «MO_x-C»*

*Carbothermal synthesis at
moderate temperatures and
reduced pressure*

The main stages of hybrid synthesis of
nanosized ultra-refractory carbides

Appearance of systems at different
synthesis stages of ultra-refractory
complex carbides



Preparation of Nanocrystalline Refractory Carbides – TiC, ZrC, HfC, TaC, Ta₄ZrC₅, Ta₄HfC₅

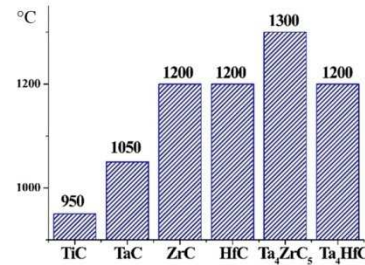
Synthesis of precursors -
alkoxides and
alkoxoacetylacetonates of
metals

Hydrolysis and gelation in
the presence of polymeric
carbon source

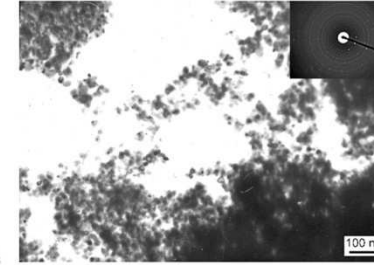
Drying of gel and preliminary
thermal treatment → the resin
pyrolysis and formation of
highly dispersed
system «MO_x-C»

Carbothermal synthesis at
moderate temperatures and
reduced pressure

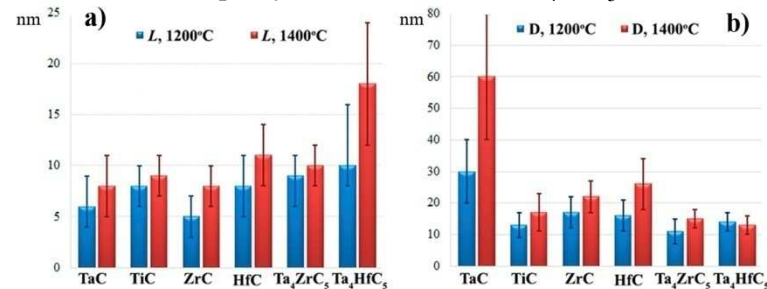
The scheme of hybrid synthetic
method for nanocrystalline
refractory carbides



Temperature of monophase
simple synthesis



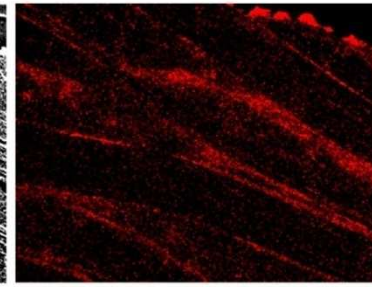
Microstructure (TEM) of the complex
carbide Ta₄HfC₅ obtained at 1200°C



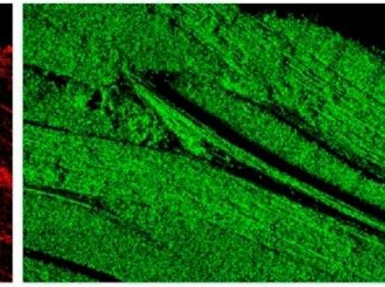
The size of crystallites (a) and size of particles according TEM
(b) of the refractory metal carbides synthesized at 1200 and 1400°C



1 mm



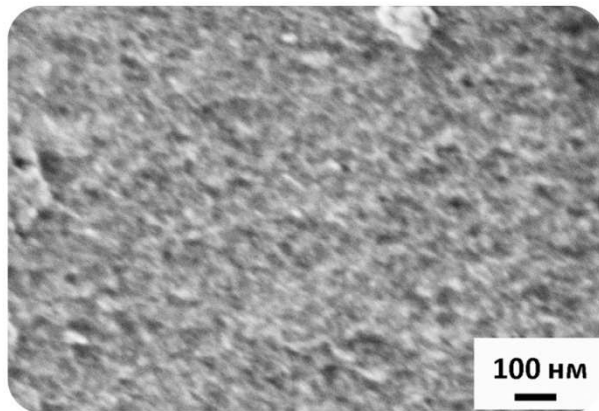
Ti Kα1



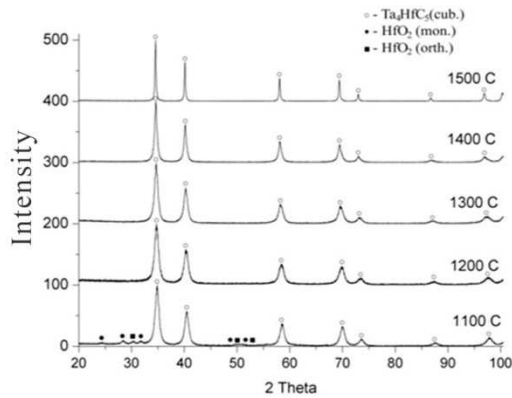
C Kα1 2

Microstructure of the cut composite material C_f/C-TiC and the
distribution thereon of titanium and carbon

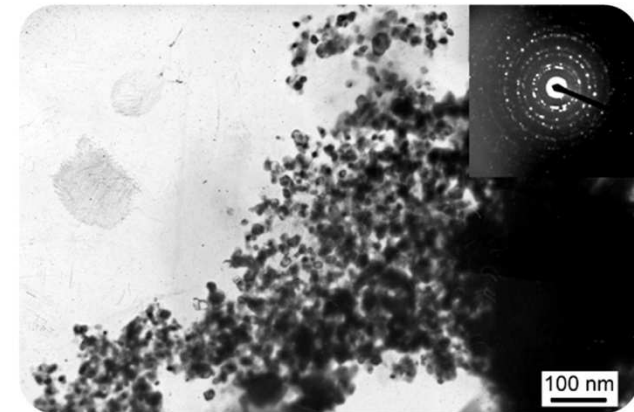
Highly Dispersed Refractory Metal Carbides TaC, TiC, ZrC, HfC, TaC-ZrC, TaC-HfC as Components for Boride Ceramic Modification



Microstructure of the particle surface
 $\text{HfO}_2\text{-Ta}_2\text{O}_5\text{-C}$



X-ray diffraction pattern of the complex carbide Ta_4HfC_5



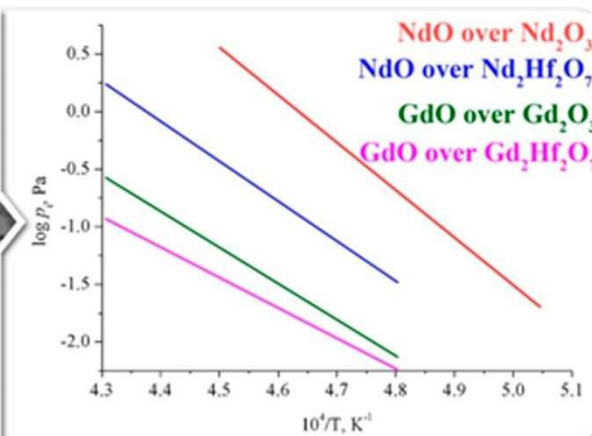
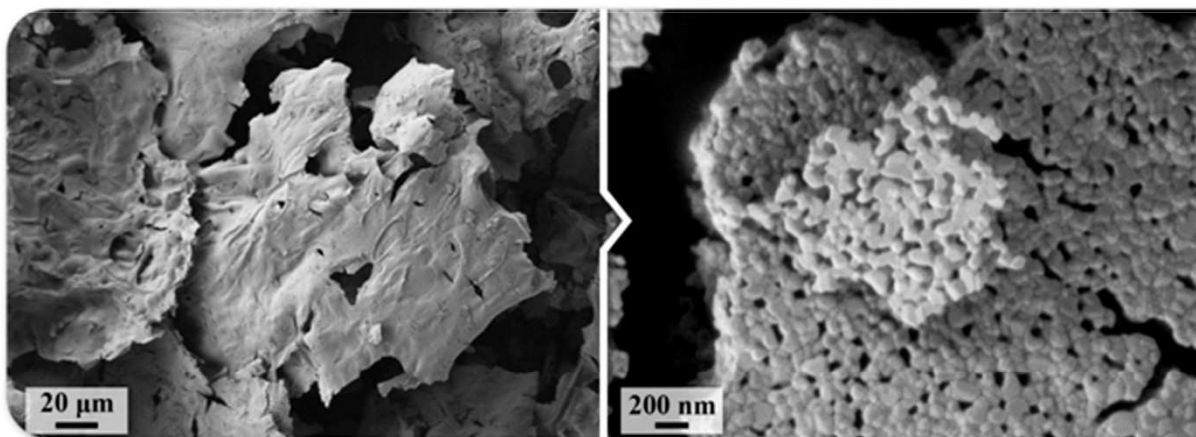
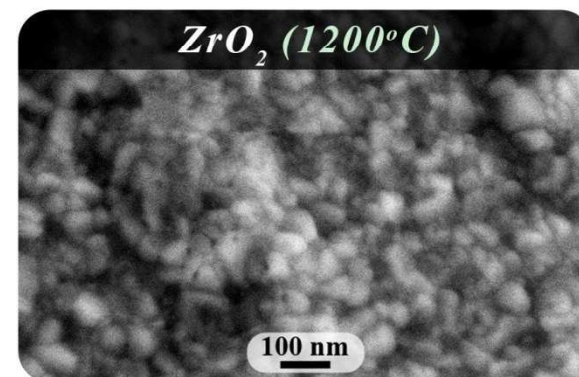
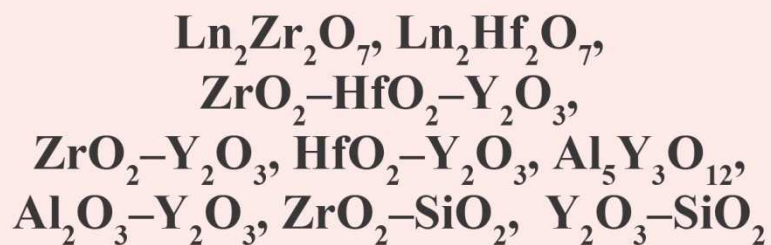
TEM of the Ta_4HfC_5 synthesized at $T=1400^\circ\text{C}$

T, °C	TaC		TiC		ZrC		HfC		Ta_4HfC_5		Ta_4ZrC_5	
	L,nm (XRD)	d,nm (TEM)	L,nm (XRD)	d,nm (TEM)	L,nm (XRD)	d,nm (TEM)	L,nm (XRD)	d,nm (TEM)	L,nm (XRD)	d,nm (TEM)	L,nm (XRD)	d,nm (TEM)
1200	6±2	30±10	8±2	13±2	5±2	17±3	8±3	16±4	10±2	14±3	9±3	11±4
1400	8±3	60±20	9±2	17±2	8±2	22±5	11±3	26±8	18±6	13±3	10±2	15±3

Highly Dispersed Refractory Metal Oxides as Components of Composite Materials

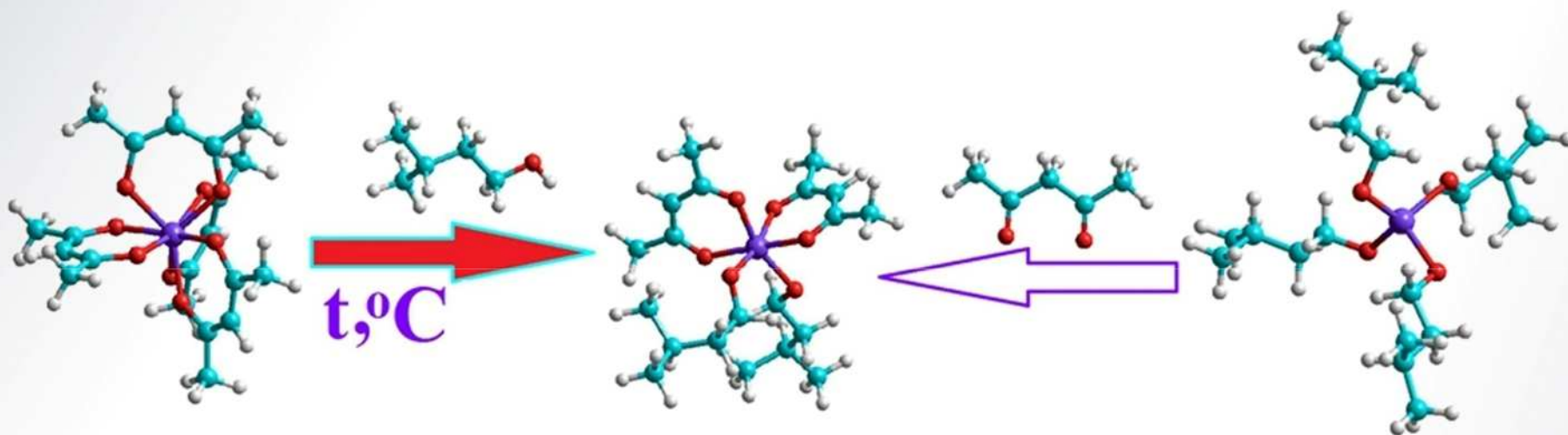
Sol-Gel method

*Glycol-citrate method
(Pechini method)*



V. G. Sevastyanov, E.P. Simonenko, N.P. Simonenko, V.L. Stolyarova, S.I. Lopatin, N.T. Kuznetsov, *European Journal of Inorganic Chemistry*. – 2013. № 26, 4636–4644

SYNTHESIS OF PRECURSORS OF NANODISPERSED METAL OXIDES AND CARBIDES POWDERS BY SOL-GEL TECHNIQUE

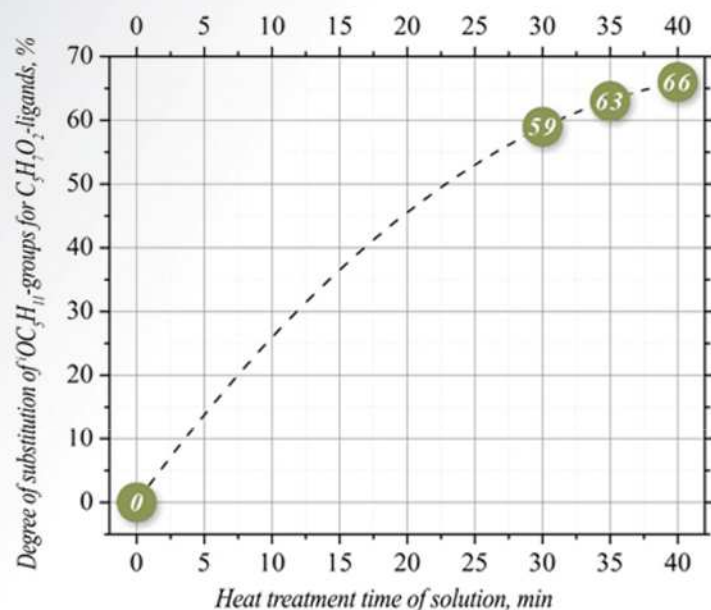


1. Hydrolytically inactive;
2. Relatively simple route of synthesis;
3. Sufficient storage stability;
4. Dosing convenience.

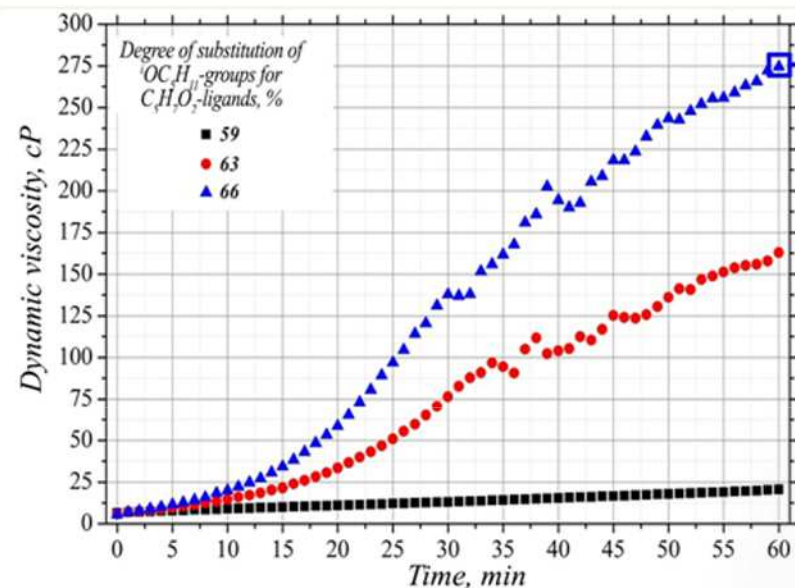
Controllable reactivity during sol-gel processes by varying the composition of the coordination sphere - alkoxide and chelating ligands ratios

1. High sensitivity to moisture, including atmospheric moisture;
2. Difficulties upon storage.

PREPARATION OF PRECURSOR SOLUTIONS OF NANOSTRUCTURED REFRACTORY MATRIX 15 mol% Y_2O_3 - 60 mol% ZrO_2 - 25 mol% HfO_2



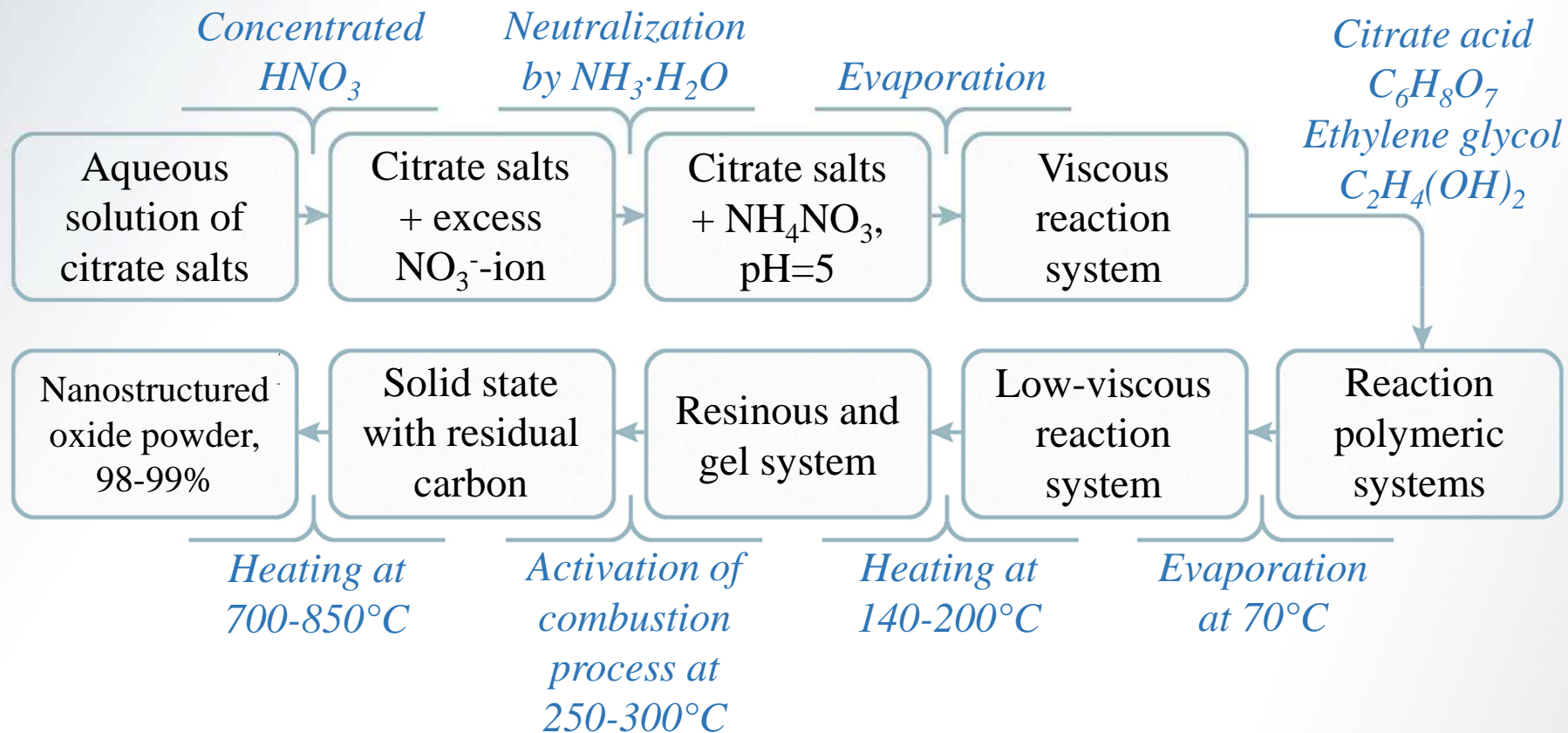
Increase in the degree of substitution of OC_5H_{11} -groups for $C_5H_7O_2$ -ligands with increasing the heat treatment time of zirconium, hafnium and yttrium acetylacetonate solution



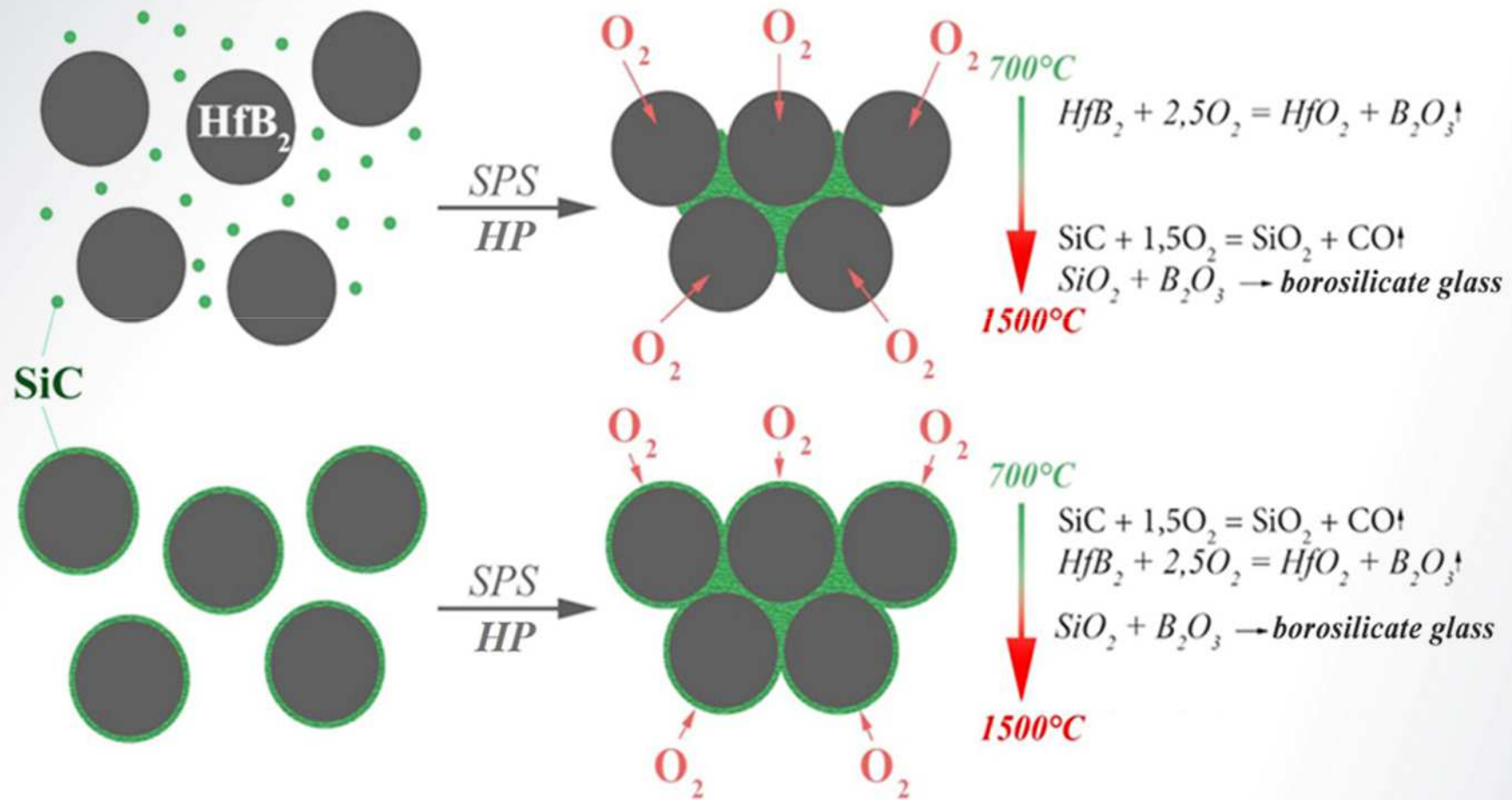
Dynamic viscosity of zirconium, hafnium and yttrium alkoxoacetylacetonates solutions with different composition of the coordination sphere during hydrolysis

*According to [V.G. Sevastyanov, E.P. Simonenko, N.P. Simonenko, V.L. Stolyarova, S.I. Lopatin, N.T. Kuznetsov, Synthesis, vaporization and thermodynamics of ceramic powders based on the Y_2O_3 - ZrO_2 - HfO_2 system // Materials Chemistry and Physics – 2015. – T. 153 – C.78–87] up to the temperature of 2500°C evaporation occurs congruently.

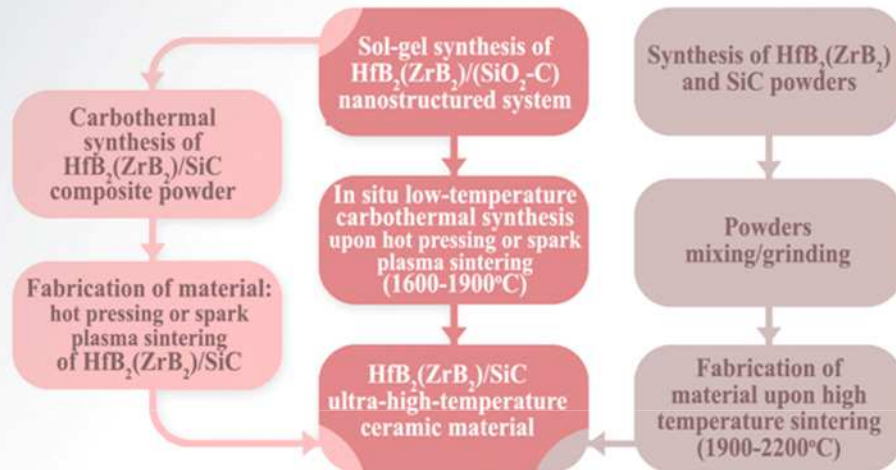
GLYCOL-CITRATE METHOD (PECHINI METHOD)



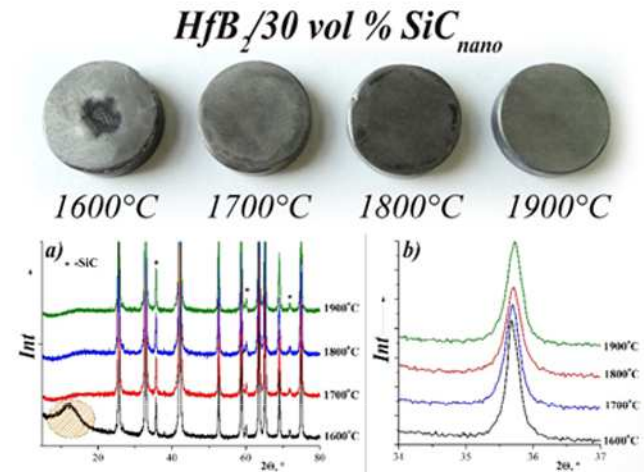
PREPARATION OF HfB_2/xSiC ($x=10\text{-}65$ vol. %) ULTRA-HIGH-TEMPERATURE CERAMIC MATERIALS



PREPARATION OF HfB_2/xSiC ($\text{x}=10\text{-}65$ vol. %) ULTRA-HIGH-TEMPERATURE CERAMIC MATERIALS



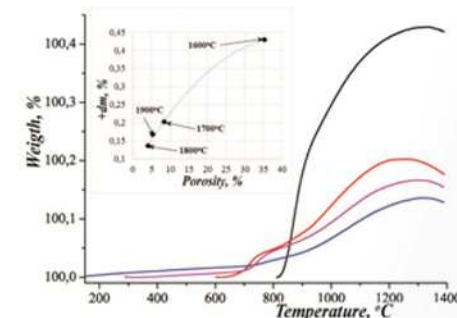
Schematic diagram of the proposed approaches (center and left) and the classical approach (right) to the manufacture of ultra-high-temperature HfB_2/SiC ceramic materials



X-ray diffraction patterns for $\text{HfB}_2/30$ vol. % SiC ultra-high-temperature ceramic composite materials, obtained at different temperatures

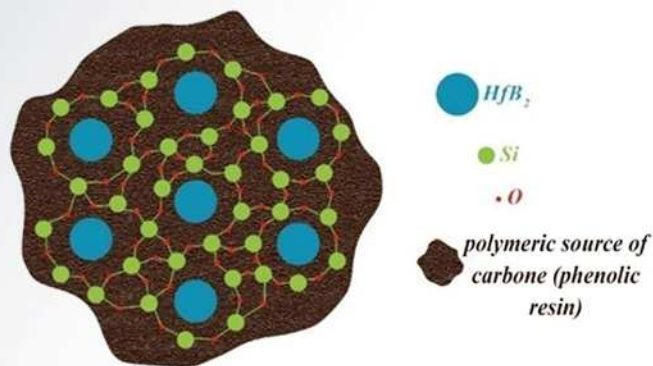
Values of density ρ , calculated porosity, linear shrinkage dI/I_0 during hot pressing, and average size of crystallites L for $\text{HfB}_2/30$ vol. % SiC ultra-high-temperature ceramics, fabricated at different temperatures

Temp., °C	ρ , g/cm ³	ρ , %	Porosity, %	dI/I_0 , %	L , nm
1600	5,35±0,50	64,4	35,6±6,0	51,2±4,0	47,6±2,6
1700	7,55±0,08	90,8	9,2±1,0	67,7±0,6	37,0±2,3
1800	7,86±0,20	94,5	5,5±2,4	68,9±0,7	35,7±1,7
1900	7,83±0,15	94,2	5,8±1,8	68,1±0,5	37,7±3,8

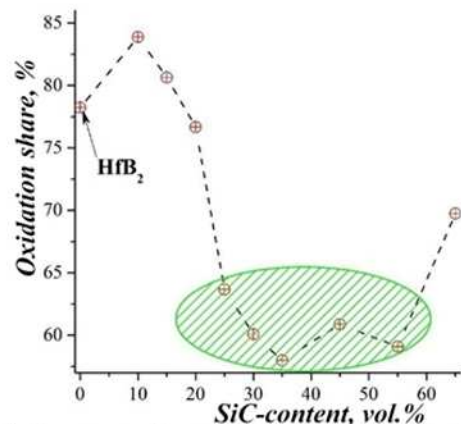


TGA curves for $\text{HfB}_2/30$ vol.% SiC samples, obtained at temperatures of 1600-1900°C, in the inset - weight gain of samples versus porosity

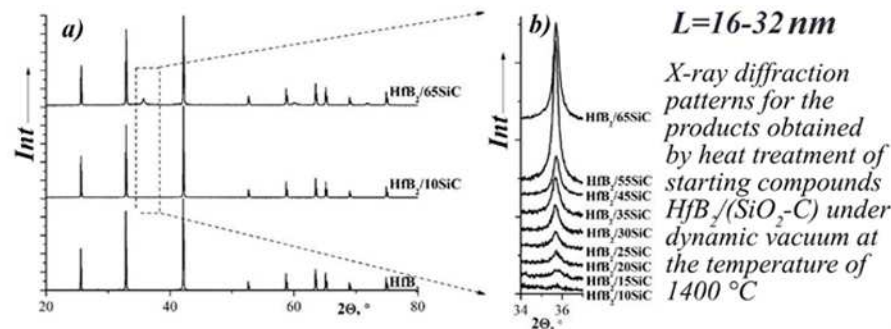
CHEMICAL MODIFICATION OF HfB_2 PARTICLES SURFACE WITH NANOCRYSTALLINE SILICON CARBIDE AND PREPARATION OF HfB_2/xSiC ($\text{x}=10\text{-}65$ vol. %) COMPOSITE POWDERS



The structure of gel, which contains hafnium diboride particles apart from silica framework and polymeric carbon source

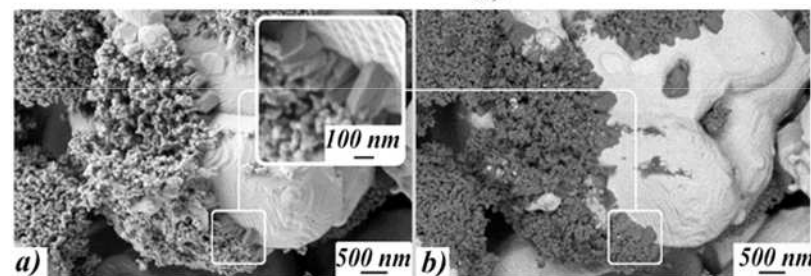


Oxidation proportion of HfB_2/xSiC ($\text{x}=0\text{-}65\text{vol.}\%$) composite powders heated in flowing air at temperatures ranging from 20 to 1400°C in comparison with total oxidation of both components

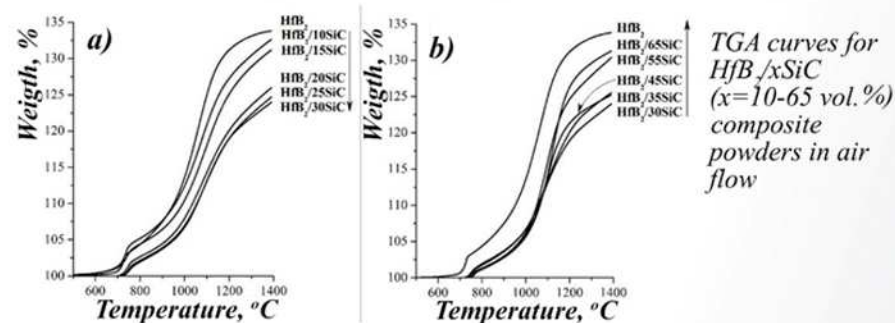


$L=16\text{-}32$ nm

X-ray diffraction patterns for the products obtained by heat treatment of starting compounds $\text{HfB}_2/(\text{SiO}_2\text{-C})$ under dynamic vacuum at the temperature of 1400 °C



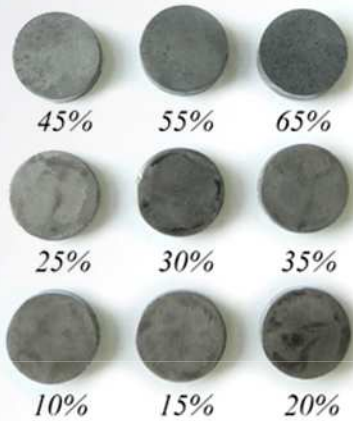
Microstructure of $\text{HfB}_2/45\text{vol.}\%\text{SiC}$ composite powder: according to the secondary electron detector (a) and in the BSE-imaging mode



TGA curves for HfB_2/xSiC ($\text{x}=10\text{-}65$ vol. %) composite powders in air flow

PREPARATION OF HfB_2/xSiC (x=10-65 vol. %) ULTRA-HIGH-TEMPERATURE CERAMIC MATERIALS

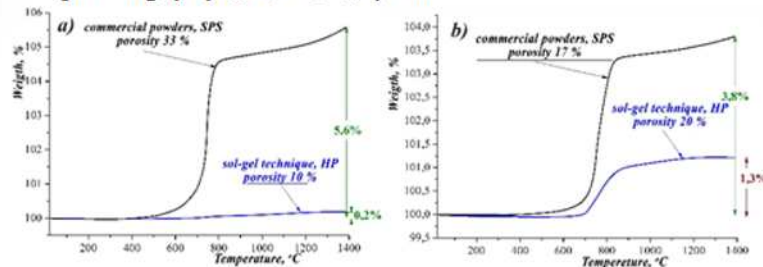
$\text{HfB}_2/\text{x vol. \% SiC}_{\text{nano}}$ (1800°C)



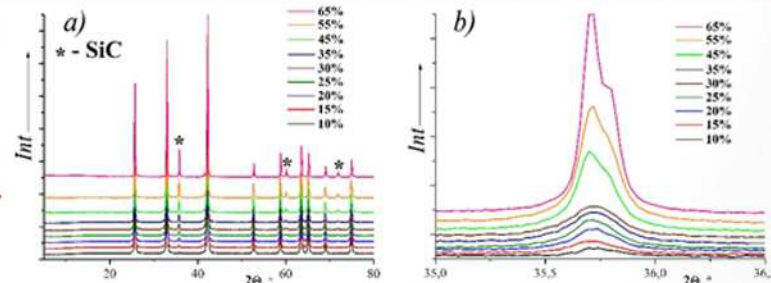
Appearance of HfB_2/xSiC (x=10-65 vol. %) ultra-high-temperature ceramic samples obtained via hot pressing of $\text{HfB}_2/\text{x}(\text{SiO}_2\text{-C})$ system

Values of density ρ , calculated porosity, linear shrinkage during hot pressing, average size of crystallites L , and weight gain under heating to 1400°C in air flow $\Delta m/m$ for HfB_2/xSiC (x=10-65 vol. %) ultra-high-temperature ceramics, fabricated at 1800°C

x, vol. % SiC	ρ , g/cm ³	ρ , %	Porosity, %	dI/I ₀ , %	L, nm	$\Delta m/m$, %
10	8,69±0,08	89,0	11,0±0,9	52,3±0,5	42,4±2,6	0,50
15	8,42±0,04	89,5	10,5±0,4	61,9±0,3	41,0±2,8	0,27
20	8,54±0,18	94,4	5,6±2,0	67,7±3,3	38,3±2,1	0,20
25	8,21±0,20	94,6	5,4±2,3	69,4±0,4	38,3±1,3	0,18
30	7,86±0,20	94,5	5,5±2,4	68,9±0,7	35,7±1,7	0,14
35	6,81±0,15	85,7	14,3±1,8	65,5±1,6	40,7±1,7	1,20
45	5,85±0,16	81,0	19,0±2,3	76,0±1,0	50,8±1,2	1,27
55	4,64±0,19	71,5	28,5±3,0	73,4±1,9	54,5±2,8	6,26
65	3,78±0,13	65,6	34,4±2,2	75,3±1,1	60,3±1,5	5,07



TGA curves for $\text{HfB}_2/\text{x vol. \% SiC}$ derived from commercially available HfB_2 and SiC powders. $\text{HfB}_2/\text{x vol. \% SiC}$ samples were fabricated by SPS method (black) and proposed technique based on the hot pressing of $\text{HfB}_2/(\text{SiO}_2\text{-C})$ (blue); x = 15 (a) and 45 (b) vol. %



X-ray diffraction patterns for $\text{HfB}_2/\text{x SiC}$ (x=10-65 vol. %) ultra-high-temperature ceramic composite materials, obtained via hot pressing of $\text{HfB}_2/\text{x}(\text{SiO}_2\text{-C})$ system

Ways to Improve the Target Properties of CM

1. Variation of the chemical composition of the CM:

- The ratio of $\text{Zr(Hf)B}_2\text{:SiC}$;
- Substitution of the SiC by alternative glass-forming compounds - Si_3N_4 , TaC, MoSi_2 , TaSi_2 and others;
- Partial substitution of the Zr(Hf)B_2 for TaB_2 , NbB_2 , VB_2 and others the oxides of which do not cause phase separation;
- Introduction in the charge the refractory oxide systems with low steam pressure and without phase transition over a wide temperature range;
- Introduction of the refractory metals, for example, iridium.

2. Establishment of dispersity effect of an initial powders on operation characteristics. The development of effective synthesis methods for refractory components of the CCM - SiC, ZrC-TaC, TaC, TaC-HfC and others.

3. Establishment of ceramic materials porosity effect on their practicality in the conditions of aerodynamic heating by dissociated airflow.

THE RESEARCH GROUP OF THE IGIC RAS



академик
Н.Т. Кузнецов



чл.-корр РАН
В.Г. Севастьянов



д.х.н. Ю.С. Езов



к.т.н. Л.А. Орлова



к.х.н. Е.П. Симоненко



к.х.н. В.С. Попов



к.х.н. Н.П. Симоненко



к.х.н. Н.А. Игнатов



асп. К.А. Сахаров



асп. В.А. Николаев



асп. А.В. Дербенёв



асп. А.С. Мокрушин



студ. Ф.Ю. Гороблов



THANKS FOR YOUR ATTENTION!